Novel Experimental Parameters to Quantify the Modulation of Absorptive and Secretory Transport of Compounds by P-Glycoprotein in Cell Culture Models of Intestinal Epithelium

Matthew D. Troutman[1] and Dhiren R. Thakker[1,2]

Received December 6, 2002; accepted April 24, 2003

Purpose. The purpose of this work was to elucidate the asymmetric effect of P-gp on modulation of absorptive and secretory transport of compounds across polarized epithelium, to develop experimental parameters to quantify P-gp-mediated modulation of absorptive and secretory transport, and to elucidate how P-gp-mediated modulation of transport is affected by passive diffusion properties, interaction of the substrate with P-gp, and P-gp expression.

Methods. The permeability of a set of P-gp substrates was determined in absorptive and secretory directions in Madine–Darby Canine kidney (MDCK), Caco-2, and MDR-MDCK monolayers. The transport was also determined in the presence of GW918, a non-competitive P-gp inhibitor, to quantify the permeability without the influence of P-gp. From these two experimental permeability values in each direction, two new parameters, absorptive quotient (AQ) and the secretory quotient (SQ), were defined to express the functional activity of P-gp during absorptive and secretory transport, respectively. Western blot analysis was used to quantify P-gp expression in these monolayers and in normal human intestinal.

Results. P-gp expression in Caco-2 and MDR-MDCK monolayers was comparable to that in normal intestine, and much less in MDCK cells. For all models, the substrates encompassed a wide range of apparent permeability due to passive diffusion (P_{PD}). The parameters AQ and SQ, calculated for all compounds, assessed the attenuation in absorptive and enhancement of secretory transport, respectively, normalized to the permeability due to passive diffusion. Analysis of these parameters showed that 1) P-gp affected absorptive and secretory transport differentially and 2) compounds could be stratified into distinct groups with respect to the modulation of their absorptive and secretory transport by P-gp. Compounds could be identified whose absorptive transport was either strongly affected or poorly affected by changes in P-gp expression. For certain compounds, AQ values showed parabolic relationship with respect to passive diffusivity, and for others AQ was unaffected by changes in passive diffusivity.

Conclusions. The relationship between attenuation of absorptive transport and enhancement of secretory transport of compounds by P-gp is asymmetric, and different for different sets of compounds. The relationship between attenuation of absorption by P-gp and passive diffusivity of compounds, their interaction potential with P-gp, and levels of P-gp expression is complex; however, compounds can be classified into sets based on these relationships. A classification system that describes the functional activity of P-gp with respect to modulation of absorptive and secretory transport was developed from these results.

KEY WORDS: P-glycoprotein; intestinal absorption; absorptive quotient; P-gp expression; passive permeability.

INTRODUCTION

Prediction of oral absorption is a complex problem and is yet to be fully understood. One factor that can add to this complexity is the apically directed efflux transporter, P-glycoprotein (P-gp), which attenuates the absorptive and enhances the secretory transport of its substrates across intestinal epithelium (1–3). Recently, it has been shown that P-gp can decrease the oral bioavailability of its substrates by attenuating intestinal absorption and by potentially enhancing intestinal metabolism of substrates that are subject to first-pass intestinal metabolism (4–14). For certain substrates, P-gp-mediated efflux activity has been shown to make intestinal exsorption (from blood into gut) an efficient route of drug elimination (15–20). Inter- and intra-patient variability in intestinal P-gp expression, possible drug-drug interactions involving co-administered P-gp substrates, inhibitors, and inducers, and the dose-dependent absorption due to saturation of P-gp can lead to dangerous and unpredictable variability in the disposition of P-gp substrates (10,21–25).

Given the potential implications of P-gp-mediated efflux activity for the intestinal disposition of its substrates, it is critical to identify novel and existing drug compounds for which this activity will play a significant role in their intestinal absorption and secretion. Although P-gp-mediated efflux activity in the intestine has been extensively studied with *in vitro* models, and these models have been successful in identifying compounds that are subject to P-gp-mediated efflux activity, the currently used models do not predict how P-gp-mediated efflux activity affects the intestinal absorption or secretion of its substrates (11,13,26–29). It was shown in previous studies that P-gp modulates transport of compounds asymmetrically during absorptive vs. secretory transport (30,31). For substrates such as the hydrophilic cationic compounds, rhodamine 123 and doxorubicin, this is true because these substrates use entirely different absorptive and secretory transport pathways (30). For substrates that primarily use the transcellular pathway during absorptive and secretory transport, this is due to differences in apparent Km values in absorptive vs. secretory direction (31). Indeed, the asymmetric effect of P-gp on absorptive vs. secretory transport in polarized epithelium is the fundamental reason why the efflux ratio (a measure of transport polarity; i.e., secretory flux/absorptive flux) does not accurately quantify how P-gp-mediated efflux activity alters absorptive or secretory transport across polarized epithelium.

In this study we propose new experimental parameters, the absorptive quotient (AQ) and the secretory quotient (SQ), which provide a direct readout of the attenuation of absorptive transport and enhancement of secretory transport, respectively, caused by P-gp-mediated efflux in a polarized epithelium. The theoretical basis and experimental design to determine these parameters are described in the present study.

[1] Division of Drug Delivery and Disposition, School of Pharmacy, The University of North Carolina at Chapel Hill, Chapel Hill, North Carolina 27599.

[2] To whom correspondence should be addressed. (e-mail: dhiren_thakker@unc.edu)

0724-8741/03/0800-1210/0 © 2003 Plenum Publishing Corporation

MATERIALS AND METHODS

Materials

The Caco-2 cell line, Caco-2 cell clone P27.7 (32), was provided by Mary F. Paine, PhD and Paul B. Watkins, MD, both of the University of North Carolina at Chapel Hill (Chapel Hill, NC, USA) and was used from passage 47 to 55. Madine-Darby canine kidney (MDCK) cells (strain II) were obtained from American Type Culture Collection (Rockville, MD, USA) and were used from passage 65 to 75. MDCK cells (strain II) transfected with human multidrug resistance P-gp (MDR1) cDNA (MDR-MDCK) were obtained from Piet Borst, PhD of The Netherlands Cancer Institute (Amsterdam, The Netherlands) and were used from passage 30 to 40. Eagle's minimum essential medium with Earle's salts and L-glutamate, and Dulbecco's modified eagle medium containing high glucose, L-glutamine, sodium pyruvate (110 mg/L), and pyridoxine HCl, were obtained from Gibco Laboratories (Grand Island, NY, USA). Fetal bovine serum, nonessential amino acids (×100), 0.05% trypsin–EDTA solution, L-glutamine 200 mM solution (×100), and penicillin–streptomycin–amphotericin B solution (×100) were obtained from Gibco Laboratories (Grand Island, NY, USA) or from Sigma Chemical Co. (St. Louis, MO, USA). Hank's balanced salt solution was obtained from Mediatech Inc., Herndon, VA. *N*-Hydroxyethylpiperazine-*N*′-2-ethanesulfonate (1 M), was obtained from Lineberger Comprehensive Cancer Center, the University of North Carolina at Chapel Hill. Transwells™ (12-mm id, 0.4-μm pore size, polycarbonate membrane) were obtained from Corning Costar (Cambridge, MA, USA). Acebutolol, colchicine, digoxin, doxorubicin, etoposide, D-(+)-glucose, D-mannitol, [^{14}C]-mannitol, methylprednisolone, prednisolone, quinidine, rhodamine 123, taxol, verapamil, and vinblastine were purchased from Sigma Chemical Co. (St. Louis, MO, USA). Ranitidine was obtained from Research Biochemicals International (Natick, MA, USA). [^{3}H]-Digoxin was obtained from New England Nuclear (Boston, MA, USA). [^{3}H]-Cyclosporin A was obtained from Amersham Pharmacia Biotech (Piscataway, NJ, USA). [^{3}H]-Taxol was obtained from Moravek Biochemicals Inc. (Brea, CA, USA). Cyclosporin A was provided by Moo J. Cho, PhD of the University of North Carolina at Chapel Hill (Chapel Hill, NC, USA). Morphine, [^{3}H]-morphine, ritonavir, [^{3}H]-ritonavir, [^{3}H]-verapamil, and [^{3}H]-vinblastine were provided by Gary M. Pollack, PhD, of the University of North Carolina at Chapel Hill (Chapel Hill, NC, USA). Talinolol was provided by Arzneimittelwerk Dresden GmbH, Radebeul, Germany. GW918 was provided by Kenneth Brouwer, PhD, GlaxoSmithKline (Research Triangle Park, NC, USA). Saquinavir was provided by Roche Discovery Welwyn, Welwyn Garden City, Hertfordshire, UK.

Cell Culture

Caco-2 Cells

Caco-2 cells were cultured as described previously (33,34). Briefly, the cells were cultured at 37°C in minimum essential medium, supplemented with 10% fetal bovine serum, 0.1 mM nonessential amino acids, 100 U/mL penicillin, 100 μg/mL streptomycin, and 0.25 μg/mL amphotericin B in an atmosphere of 5% CO_2 and 90% relative humidity. The cells were passaged upon reaching approximately 80-90% confluence using trypsin-EDTA, and plated at densities of 1:5, 1:10, or 1:20 in 75 cm^2 T-flasks. Caco-2 cells were seeded at a density of 60,000 cells/cm^2 on polycarbonate membranes of Transwells™. The culture medium was changed the day after seeding, and every other day thereafter. Medium was added to both apical (AP) and basolateral (BL) compartments. Monolayers were used approximately 21 days postseeding.

MDCK Cells

MDCK cells were cultured as previously described (35). Briefly, MDCK cells were cultured using procedures outlined for Caco-2 cells with the following modifications: (1) the cells were passaged every other day using trypsin-EDTA, and plated at a density of 1×10^5 cells per 75-cm^2 T-flask, (2) the cells were seeded at a density of 100,000 cells/cm^2 on Transwells™, and (3) the cell monolayers were used 5–7 days postseeding.

MDR-MDCK Cells

The culturing conditions used for MDR-MDCK cells were optimized for maximal P-gp functional activity and desirable passive permeability properties. MDR-MDCK cells were cultured at 37°C in Dulbecco's modified eagle medium (high glucose), supplemented with 10% fetal bovine serum, 0.1 mM% nonessential amino acids, 1% L-glutamine, 100 U/mL penicillin, 100 μg/mL streptomycin, and 0.25 μg/mL amphotericin B in an atmosphere of 5% CO_2 and 90% relative humidity. The cells were passaged every other day using trypsin-EDTA, and plated at a density of 750,000 cells per 75-cm^2 T-flask. MDR-MDCK cells were seeded at a density of 200,000 cells/cm^2 on Transwells™. Medium was changed the day after seeding, and every other day thereafter. Medium was added to both AP and BL compartments. The cell monolayers were used 5 or 6 days postseeding.

Western Blot Analysis of P-gp

P-gp expression levels were quantified for Caco-2, MDCK, and MDR-MDCK cell monolayers, and for human intestinal homogenates from the duodenum, jejunum, and ileum of a single normal volunteer using a method described by Paine *et al.* (25). Human intestinal homogenates from the samples representing the duodenum, jejunum, and ileum, obtained at 2-, 8-, and 14-foot regions of the gastrointestinal tract of a healthy 21-year-old female, respectively, were provided by Mary F. Paine, PhD, of the University of North Carolina at Chapel Hill (Chapel Hill, NC, USA). For Caco-2, MDCK, and MDR-MDCK cell monolayers, the polycarbonate membrane of the Transwell™ insert was excised using a razor blade and the monolayer was lysed in 100 μL of ice-cold lysis buffer containing 20% glycerol, 0.1 M Tris-HCl, 10 mM EDTA, 1 mM dithiothreitol, 1 mM phenylmethylsulfonyl fluoride, 1 mM benzamidine, and 1 μg/mL aprotinin (pH 7.4) for 2 h—this was performed in triplicate to yield three samples per cell type. Total protein content was quantified according to Lowry *et al.* (36), with bovine serum albumin as the reference standard. All samples were diluted in sample

buffer consisting of 2% sodium dodecyl sulfate, 5% sucrose, 5% 2-mercaptoethanol, and 50 mM Tris-HCl (pH 6.8) to final concentration of 15 μg protein/60 μL. Samples (15 μg protein/well) were separated electrophorectically and then transferred overnight to a 0.45-μm pore size polyvinylidene diflouride membrane. P-gp was detected with a primary rabbit polyclonal antibody from the laboratory of Erin G. Schuetz, PhD, of St. Jude's Children's Research Hospital (Memphis, TN, USA) and a Horseradish peroxidase conjugated goat anti-rabbit IgG/A/M (Zymed Laboratories, San Francisco, CA, USA) secondary antibody. P-gp was exposed using chemiluminescence reagents (Amersham Biosciences, Inc; Piscataway, NJ, USA.). The Chemi-Doc imaging system (Bio-Rad, Hercules, CA, USA) was used to visualize P-gp. Band intensities were assessed by densitometric analysis performed using version 4.1 of the Quantity One imaging software (Bio-Rad), and P-gp expression was quantified by integrated optical density (IOD).

Substrate Transport across Cell Monolayers under Normal Conditions and in the Presence of GW918

Cell monolayers were incubated in transport buffer (TBS: Hanks balanced salt solution with 25 mM D-glucose and 10 mM *N*-Hydroxyethylpiperazine-*N*′-2-ethanesulfonate, pH 7.4) with 1% (v/v) dimethylsulfoxide for 30 min at 37°C (temperature maintained throughout the experiment). To ensure Caco-2 and MDCK cell monolayer integrity, the transepithelial electrical resistance (TEER) was measured using an EVOM Epithelial Tissue Voltammeter and an Endohm-12 electrode (World Precision Instruments, Sarasota, FL, USA). Caco-2 and MDCK cell monolayers with TEER values ≥ 300 $\Omega \cdot cm^2$ and ≥ 150 $\Omega \cdot cm^2$, respectively, were used for transport experiments. Donor solutions consisting of test compound with 1% (v/v) dimethylsulfoxide in TBS were added to the donor compartment—for absorptive (AP to BL) transport, donor is AP compartment, and for secretory (BL to AP) transport, donor is BL compartment. For cyclosporin A, digoxin, mannitol, morphine, ritonavir, taxol, verapamil, and vinblastine, 0.1 μCi/ml of the radiolabeled compound was added to the donor solution. Studies were performed at subsaturating concentrations (determined in preliminary experiments and in previous work) (30,31). Transport for each condition was measured in both directions (absorptive and secretory) when flux was linearly related to time (i.e., after the lag phase if present) under sink conditions (less than 10% of the initial compound added to the donor compartment at $t = 0$ min appearing in the acceptor side at the completion of the experiment). At the completion of all experiments performed in Caco-2 and MDCK cell monolayers, TEER was measured to ensure that cell monolayer integrity and viability had not been adversely affected by the experimental conditions. Data generated in Caco-2 and MDCK monolayers with final TEER ≤ 300 $\Omega \cdot cm^2$ and ≤ 150 $\Omega \cdot cm^2$, respectively, were not accepted. To ensure that MDR-MDCK cell monolayers were intact, transport of [^{3}H]-mannitol was measured over the timescale of the experiment in representative monolayers from the batch of MDR-MDCK monolayers. Data obtained from batches of MDR-MDCK cells in which mannitol apparent permeability (P_{app}) was $\geq 6 \times 10^{-7}$ cm/sec were not accepted. The absorptive P_{app} ($P_{app,AB}$) and secretory P_{app} ($P_{app,BA}$; see Eq. 2) were determined using these experimental conditions.

To determine the transport of substrates without the influence of P-gp-mediated efflux activity, absorptive and secretory transport was measured as described above in the presence of 1 μM GW918 (approx. 30-fold greater than the reported K_i for inhibition of P-gp-mediated efflux activity; Ref. 37) added to incubation, donor, and acceptor solutions. The P_{app} determined in the presence of 1 μM GW918 provided an estimate of the permeability attributed to the passive diffusion of the compound (P_{PD}) across cell monolayers. The P_{app} of theophylline, a marker for passive transcellular P_{app} in polarized epithelium (38), was unaltered in the presence of 1 μM GW918, showing GW918 does not affect passive transcellular P_{app}. P_{PD} values (in absorptive and secretory directions) were determined using these experimental conditions.

To determine the absorptive transport of substrates across MDR-MDCK cell monolayers in the presence of GW918 (45 or 85 nM), transport was measured as described above in the presence of GW918 added to incubation, donor, and acceptor solutions. Using these experimental conditions, substrate $P_{app,AB}$ across MDR-MDCK monolayers in the presence of 45 or 85 nM GW918 was determined.

Sample Analysis

Rhodamine 123 samples were analyzed by measuring fluorescence with a LS 50B Luminescence Spectrometer (Perkin–Elmer, Norwalk, CT, USA) set to excitation wavelength of 500 nm and emission wavelength of 525 nm. Radiolabeled cyclosporin A, digoxin, mannitol, ritonavir, taxol, verapamil, and vinblastine samples were analyzed using liquid scintillation counting (1600 TR Liquid Scintillation Analyzer, Packard Instrument Company, Downers Grove, IL, USA).

Acebutolol, colchicine, doxorubicin, etoposide, methylprednisolone, prednisolone, quinidine, ranitidine, saquinavir, and talinolol samples were analyzed by HPLC (Hewlett Packard, 1100 series, Wald bronn, Germany), with 100 × 3 mm Aquasil, 100 × 3 BDS Hypersil, or 100 × 1 mm Kromasil columns, all with 5 μM stationary phase (Keystone Scientific, Inc.) and with isocratic elution. Specific high-performance liquid chromatography conditions are as follows. Acebutolol and talinolol: Aquasil column, mobile phase 80:20 25 mM phosphate buffer, pH 3.5: acetonitrile, 0.75 mL/min flow rate, detection at 234 nm, retention time (rt) approx. 2.7 min (acebutolol) and approx. 2.2 min (talinolol). Colchicine: Kromasil column, mobile phase 27.5:72.5 25 mM phosphate buffer, pH 3.5: acetonitrile, 0.25 mL/min flow rate, detection at 244 nm, and rt approx. 1.8 min. Etoposide: Aquasil column, mobile phase 35:65 25 mM phosphate buffer, pH 3.5: acetonitrile, 0.75 mL/min flow rate, detection at 284 nm, and rt approx. 1.7 min. Methylprednisolone and prednisolone: BDS Hypersil column, mobile phase 50:35:15 0.1% H_3PO_4: acetonitrile: methanol, 0.75 mL/min flow rate, and detection at 246 nm, rt approx. 2.9 min (methylprednisolone) and ~2.8 min (prednisolone). Quinidine: BDS column, mobile phase 27.5:72.5 25 mM phosphate buffer, pH 3.5: acetonitrile, 0.75 mL/min flow rate, detection at 247 nm, rt approx. 2.8 min. Ranitidine: Aquasil column, mobile phase 75:25 pH 6.0 50 mM phosphate buffer: methanol, flow rate 1.0 mL/min, detection at 320 nm, and rt approx. 5.7 min. Saquinavir: BDS Hypersil column, mobile phase 42.5:57.5 pH 6.5 50 mM phosphate buffer: acetonitrile, flow rate 0.75 mL/min, detection at 238 nm, and rt approx. 3.2 min.

Data Analysis

Transport Experiments

Flux was calculated using Eq. (1):

$$J = \frac{dQ}{dt} \tag{1}$$

where Q is the amount of compound transported over time t of the experiment. Eq. (2) was used to determine the P_{app} from the flux:

$$P_{app} = \frac{J}{A \cdot C_D} \tag{2}$$

where C_D is the initial concentration of the test compound added to the donor compartment, and A is the surface area of the porous membrane in cm^2.

Statistical Analysis

Statistical analysis for significant differences was performed using the two-tailed Student's t test and assuming homoscedacity. The criterion for significant differences in values was $p < 0.05$.

Nonlinear Regression Analysis

Nonlinear regression analysis was performed using WinNonlin nonlinear regression analysis software (PharSight Corporation, Mountain View, CA, USA). Parameter estimates obtained from nonlinear regression analysis were reported ± standard error.

THEORY

Absorptive Quotient (AQ) and Secretory Quotient (SQ)

It has been previously demonstrated (31,39) that $P_{app,AB}$ and $P_{app,BA}$ can be described by Eqs. (3) and (4), respectively:

$$P_{app,AB} = P_{PD,AB} - P_{P\text{-}gp,AB} \tag{3}$$

$$P_{app,BA} = P_{PD,BA} + P_{P\text{-}gp,BA} \tag{4}$$

where $P_{P\text{-}gp}$ is the permeability due to P-gp-mediated efflux activity ($P_{P\text{-}gp,AB}$ for absorptive transport and $P_{P\text{-}gp,BA}$ for secretory transport) and P_{PD} ($P_{PD,AB}$ and $P_{PD,BA}$) is the P_{app} (Eq. 2) determined in the presence of GW918 (1 μM). The arithmetic difference between the P_{PD} and $P_{app,AB}$ values provided an estimate of the contribution of P-gp in attenuating the permeability of the compounds in the absorptive direction ($P_{P\text{-}gp,AB}$); similarly, the arithmetic difference between the $P_{app,BA}$ and P_{PD} values gave an estimate of P-gp's contribution in enhancing the permeability of compounds in the secretory direction ($P_{P\text{-}gp,BA}$). Our evidence and previous reports show that $P_{P\text{-}gp,AB}$ and $P_{P\text{-}gp,BA}$ are completely described by one-site Michaelis-Menten saturable kinetics for several structurally diverse P-gp substrates (31,39–43). $P_{P\text{-}gp,AB}$ can be calculated from the experimentally determined values, $P_{app,AB}$ and P_{PD}, measured under normal conditions and in the presence of an inhibitory concentration (concentration that completely abolishes P-gp-mediated efflux activity) of a P-gp inhibitor (e.g., 1 μM GW918), respectively. Similarly, $P_{P\text{-}gp,BA}$ can be calculated from the experimentally determined values, $P_{app,BA}$ and P_{PD}. The specificity of the inhibitor determines how accurately $P_{P\text{-}gp}$ can be calculated; however, an inhibitor with a broad selectivity for inhibition of several efflux pumps can provide an estimate of the combined effect of multiple efflux mechanisms. Importantly, when saturable processes other than P-gp (those not completely inhibited by the concentration of the inhibitor used to determine P_{PD}) affect transport of the substrate, permeability due to these saturable processes will be included in the P_{PD} term. Furthermore, when P_{PD} determined in the absorptive and secretory directions are significantly different (presumably due to the presence of additional saturable processes), we recommend using P_{PD} determined in absorptive direction in Eq. (3), and P_{PD} determined in secretory direction in Eq. (4).

To quantify and express how P-gp-mediated efflux activity affects substrate transport across polarized epithelium (i.e., the functional activity of P-gp), we have proposed two new parameters, the absorptive quotient (AQ) and the secretory quotient (SQ). AQ and SQ are described by Eqs. (5) and (6), respectively:

$$AQ = \frac{P_{PD} - P_{app,AB}}{P_{PD}} = \frac{P_{P\text{-}gp,AB}}{P_{PD}} \tag{5}$$

$$SQ = \frac{P_{app,BA} - P_{PD}}{P_{PD}} = \frac{P_{P\text{-}gp,BA}}{P_{PD}} \tag{6}$$

For the same reasons listed for Eqs. (3) and (4), we recommend using P_{PD} determined in absorptive ($P_{PD,AB}$) or secretory ($P_{PD,BA}$) direction in Eqs. (5) and (6) when these values are significantly different from one another. The $P_{P\text{-}gp,AB}$ and $P_{P\text{-}gp,BA}$ values, when normalized to P_{PD} values, numerically express the effect P-gp would have in attenuating absorptive transport (AQ) or enhancing secretory transport (SQ) of its substrates, respectively. More specifically, AQ quantifies the functional activity of P-gp observed during absorptive transport, and SQ quantifies the functional activity of P-gp observed during secretory transport. For example, if an AQ of 0.5 is generated for a compound, this means that P-gp-mediated efflux activity attenuates the P_{PD} of this compound during absorptive transport by 50%. Similarly, if an SQ value of 2.0 is generated for a compound, this means that P-gp-mediated efflux activity enhances the P_{PD} of this compound during secretory transport by 2-fold.

Quantifying How Changes in P-gp Expression Affect AQ: Titration of P-gp-Mediated Efflux Activity with GW918 and Determination of IC_{50} (AQ)

To directly elucidate how changes in P-gp expression affect the functional activity of P-gp during absorptive transport, an experimental strategy was conceived to simulate P-gp expression changes while keeping other determinants, such as substrate P_{PD} and interaction with P-gp, constant; thus avoiding model dependent differences in the determinants of the functional activity of P-gp. MDR-MDCK monolayers were used for this approach due to their short culture time and high expression of MDR1 gene product P-gp—it was expected that the level of P-gp expression in this cell line would correlate to the highest P-gp expression that might be observed *in vivo*. Changes in P-gp expression affect the J_{max} of P-gp-mediated efflux activity (an activity described by one-site saturable kinetics). By using the noncompetitive P-gp inhibitor GW918

(37,44) it was possible to systematically titrate down (reduce) J_{max} for P-gp-mediated efflux activity, analogous to reducing P-gp expression.

To assess how the functional activity of P-gp during absorptive transport (AQ) decreased in response to decreasing Jmax, we have defined the term IC_{50} (AQ). This value is the concentration of the noncompetitive P-gp inhibitor, GW918 that caused a 50% reduction in AQ. The IC_{50} (AQ) was calculated from AQ values determined under normal conditions, and in the presence of 45 and 85 nM GW918 in MDR-MDCK cell monolayers using nonlinear regression analysis with Eq. (7):

$$AQ = AQ_{max} \cdot \left[1 - \left(\frac{[GW918]}{[GW918] + IC_{50}(AQ)}\right)\right] \quad (7)$$

where AQ_{max} is the AQ determined under normal conditions.

RESULTS

P-gp Expression in Normal Human Intestine and in Caco-2, MDCK, and MDR-MDCK Cell Monolayers

P-gp expression was quantified by Western blot analysis to assess the level of P-gp expression in the three cell culture models of polarized epithelium (Caco-2, MDCK, and MDR-MDCK cell monolayers) used in these studies with respect to the P-gp expression in the duodenal, jejunal, and ileal regions of normal human intestine (Fig. 1). It has been observed that P-gp expression in the normal human intestine generally increases from duodenum to ileum; however, these regional differences in expression are slight (25). As expected, P-gp expression was marginally greater in ileum vs. duodenum. Interestingly, expression observed for the jejunal sample was approximately 2-fold greater than that observed for duodenal or ileal samples. For each cell culture model, P-gp expression was relatively constant between samples, with ~15% deviation in expression observed between individual samples per cell type. P-gp expression in MDCK cell monolayers was very low, and was much lower than that observed in the human intestinal samples and in Caco-2 and MDR-MDCK cell monolayers. Although this finding was expected (45,46), these results must be interpreted with caution because of the fact that the primary antibody used to detect P-gp was raised against a peptide of human P-gp (25), and MDCK cell monolayers solely express canine P-gp. Expression observed for Caco-2 and MDR-MDCK cell monolayers was within the range of expression observed for the human intestinal samples. Caco-2 cell monolayer expression was comparable to expression observed in duodenum and ileum but approx. 2-fold less than that observed in jejunum. MDR-MDCK cell monolayer expression was intermediate between expression observed in duodenum and ileum, and expression observed in jejunum. MDR-MDCK cell monolayer P-gp expression was slightly greater than that observed for Caco-2 cell monolayers.

Absorptive and Secretory Permeability of P-gp Substrates in Epithelial Cell Culture Models

The apparent permeability values in the absorptive direction, $P_{app,AB}$, in Caco-2, MDR-MDCK, and MDCK cell monolayers for a set of P-gp substrates, containing compounds of wide chemical diversity, are listed in Tables I, II, and III, respectively. Similarly, the apparent permeability values in the secretory direction, $P_{app,BA}$, in the same cell culture models are listed in Table IV. The permeability of these compounds was also determined after complete inhibition of P-gp with the non-competitive inhibitor of P-gp, GW918. These permeability values were attributed to the transport of the compounds via the passive diffusion process, and are designated as P_{PD}. Generally, the P_{PD} values determined in the absorptive and secretory directions were statistically equal. The $P_{app,BA}$ values were greater than $P_{app,AB}$ values, and for nearly all substrates (except doxorubicin, morphine, ranitidine, and rhodamine 123), $P_{app,AB}$ values were lower than the P_{PD} values, consistent with P-gp's role in attenuating absorptive transport of its substrates. The P_{PD} values of the substrates spanned a range of 1.5 to 2 log units in each cell culture model. Interestingly, P_{PD} values determined in MDR-MDCK cell monolayers were smaller for all substrates (except doxorubicin) than those determined in Caco-2 cell monolayers.

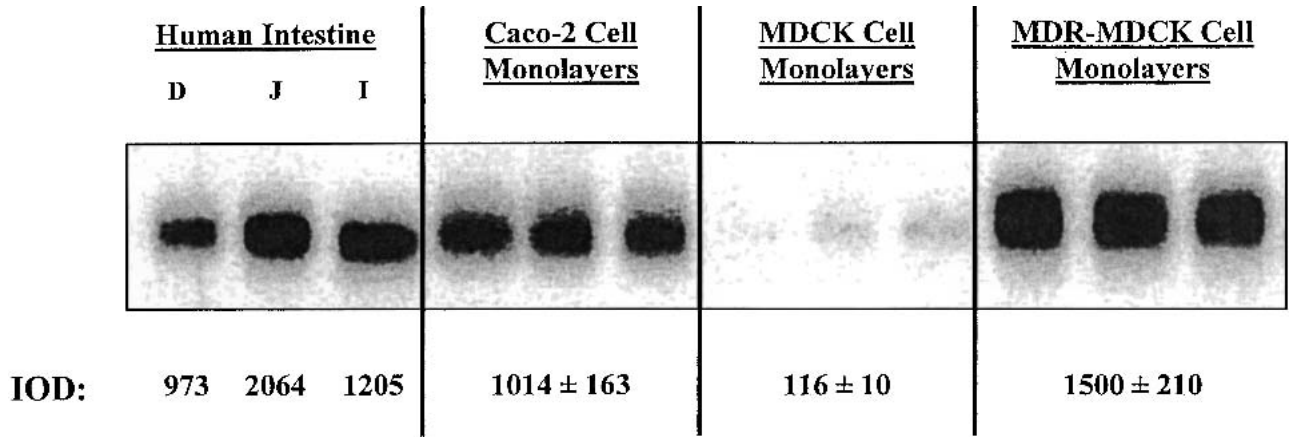

Fig. 1. Western blot analysis of P-gp expression in human intestine and Caco-2, MDCK, and MDR-MDCK monolayers. For human intestine, duodenum, jejunum, and ileum samples were taken at 2, 8, and 14 feet along the gastrointestinal tract, respectively. For each lane, 15 μg total protein was loaded. The western blot analysis was performed as described in Materials and Methods section. P-gp expression was quantified by integrated optical densitometry (IOD) analysis (n = 1).

Table I. $P_{app,AB}$, P_{PD}, and AQ Values, and Efflux Ratios Generated for P-glycoprotein Substrates in Caco-2 Cell Monolayers

Substrate (μM)	$P_{app,AB}$[a] (cm/s) × 10^6	P_{PD}[b] (cm/s) × 10^6	AQ	Efflux ratio[c]
Acebutolol (20 μM)	1.52 ± 0.14	6.36 ± 1.81	0.76 ± 0.24	12.1 ± 1.1
Colchicine (25 μM)	1.00 ± 0.24	2.76 ± 0.73	0.64 ± 0.35	16.9 ± 4.0
Cyclosporin A (0.1 μM)	3.02 ± 0.22	6.85 ± 0.16	0.56 ± 0.06	5.7 ± 0.6
Digoxin (10 μM)	2.18 ± 0.10	14.9 ± 1.84	0.85 ± 0.15	20.2 ± 1.0
Doxorubicin (10 μM)	0.57 ± 0.11	0.57 ± 0.28	0.00 ± 0.38	26.5 ± 3.0
Etoposide[d] (25 μM)	1.12 ± 0.11	3.03 ± 0.19	0.63 ± 0.08	12.5 ± 1.5
Methylprednisolone (20 μM)	10.5 ± 0.40	41.9 ± 4.81	0.75 ± 0.16	7.8 ± 0.5
Morphine (1 μM)	16.7 ± 1.30	16.8 ± 0.85	0.01 ± 0.10	1.3 ± 0.1
Prednisolone (20 μM)	25.5 ± 1.46	35.9 ± 1.34	0.21 ± 0.06	3.4 ± 0.2
Quinidine (1 μM)	20.8 ± 0.32	55.9 ± 0.99	0.63 ± 0.06	5.2 ± 0.2
Ranitidine (100 μM)	2.73 ± 0.16	2.84 ± 0.74	0.04 ± 0.22	1.6 ± 0.2
Rhodamine 123 (10 μM)	1.42 ± 0.30	1.73 ± 0.29	0.18 ± 0.22	11.4 ± 2.6
Ritonavir (0.1 μM)	5.57 ± 0.49	9.33 ± 1.80	0.40 ± 0.18	7.3 ± 0.8
Saquinavir (20 μM)	4.74 ± 1.60	18.2 ± 0.28	0.74 ± 0.18	16.9 ± 5.8
Talinolol[d] (20 μM)	6.69 ± 0.15	14.9 ± 0.15	0.55 ± 0.02	4.4 ± 0.1
Taxol[d] (10 μM)	1.77 ± 0.14	17.9 ± 0.59	0.90 ± 0.05	41.9 ± 0.2
Verapamil (0.1 μM)	44.5 ± 3.53	86.3 ± 3.47	0.48 ± 0.07	2.6 ± 0.2
Vinblastine (0.1 μM)	3.07 ± 0.44	17.7 ± 3.11	0.83 ± 0.23	14.1 ± 2.1

[a] $P_{app,AB}$ values represent the mean of no less than three determinations ± SD.
[b] P_{PD} values represent the average of no less than three determinations performed in both absorptive and secretory directions, respectively, ± SD. P_{PD} values in absorptive and secretory directions were not significantly different at $\alpha = 0.1$, except where noted.
[c] $P_{app,BA}$ values determined in Caco-2 monolayers shown in Table IV were used to calculate efflux ratios.
[d] P_{PD} values determined in absorptive and secretory directions were significantly different ($\alpha < 0.1$), and P_{PD} determined in absorptive direction are shown. P_{PD} values are reported as the mean of no less than three determinations ± SD.

Table II. $P_{app,AB}$, P_{PD}, and AQ Values Generated for P-glycoprotein Substrates in MDR-MDCK Cell Monolayers

Substrate (μM)	$P_{aap,AB}$[a] (cm/s) × 10^6	P_{PD}[b] (cm/s) × 10^6	AQ
Acebutolol (20 μM)	0.56 ± 0.15	3.73 ± 0.23	0.85 ± 0.10
Colchicine (25 μM)	0.64 ± 0.23	1.64 ± 0.26	0.61 ± 0.28
Cyclosporin A (0.1 μM)	0.65 ± 0.17	4.32 ± 0.58	0.85 ± 0.12
Digoxin (10 μM)	1.89 ± 0.13	7.50 ± 0.66	0.75 ± 0.11
Doxorubicin (10 μM)	0.87 ± 0.22	0.82 ± 0.23	0.00 (–0.06 ± 0.32)
Etoposide (25 μM)	0.30 ± 0.09	0.66 ± 0.19	0.54 ± 0.20
Methylprednisolone (20 μM)	6.43 ± 0.25	28.48 ± 4.42	0.77 ± 0.18
Morphine (1 μM)	7.22 ± 0.77	8.62 ± 1.15	0.16 ± 0.15
Prednisolone (20 μM)	14.6 ± 5.50	27.22 ± 1.24	0.46 ± 0.22
Quinidine (1 μM)	10.4 ± 0.97	31.7 ± 0.96	0.67 ± 0.09
Ranitidine (100 μM)	1.18 ± 0.26	1.25 ± 0.06	0.06 ± 0.21
Rhodamine 123 (10 μM)	0.98 ± 0.06	1.16 ± 0.10	0.16 ± 0.10
Ritonavir[c] (0.1 μM)	1.88 ± 0.12	3.91 ± 0.24	0.52 ± 0.08
Saquinavir[c] (20 μM)	1.72 ± 0.10	12.6 ± 5.07	0.86 ± 0.53
Talinolol (20 μM)	0.72 ± 0.07	2.69 ± 0.26	0.73 ± 0.18
Taxol[c] (10 μM)	1.49 ± 0.33	7.33 ± 0.64	0.80 ± 0.12
Verapamil (0.1 μM)	18.0 ± 1.61	35.2 ± 1.34	0.49 ± 0.07
Vinblastine[c] (0.1 μM)	0.50 ± 0.13	4.34 ± 0.73	0.89 ± 0.23

[a] $P_{app,AB}$ values represent the mean of no less than three determinations ± SD.
[b] P_{PD} values represent the average of no less than three determinations performed in absorptive and secretory directions, respectively, ± SD. P_{PD} values in absorptive and secretory directions were not significantly different at $\alpha = 0.1$, except where noted.
[c] P_{PD} values determined in absorptive and secretory directions were significantly different ($\alpha < 0.1$), and P_{PD} determined in absorptive direction are shown. P_{PD} values are reported as the mean of no less than three determinations ± SD.

Table III. $P_{app,AB}$, P_{PD}, and AQ Values Generated for *P*-Glycoprotein Substrates in MDCK Cell Monolayers

Substrate (μM)	$P_{app,AB}$[a] (cm/s) × 10^6	P_{PD}[b] (cm/s) × 10^6	AQ
Acebutolol (20 μM)	1.85 ± 0.27	2.79 ± 0.71	0.34 ± 0.33
Colchicine (25 μM)	1.03 ± 0.29	1.36 ± 0.03	0.24 ± 0.22
Cyclosporin A[c] (0.1 μM)	2.62 ± 0.13	3.75 ± 0.25	0.301 ± 0.08
Digoxin (10 μM)	1.63 ± 0.09	3.47 ± 0.14	0.53 ± 0.08
Doxorubicin (10 μM)	1.51 ± 0.55	1.15 ± 0.78	0.00 (–0.32 ± 0.57)
Etoposide (25 μM)	0.96 ± 0.18	1.42 ± 0.15	0.32 ± 0.16
Methylprednisolone (20 μM)	12.2 ± 3.04	17.1 ± 1.56	0.29 ± 0.21
Prednisolone (20 μM)	8.70 ± 0.30	10.8 ± 0.99	0.19 ± 0.11
Quinidine (1 μM)	36.8 ± 6.44	63.8 ± 7.78	0.42 ± 0.15
Rhodamine 123 (10 μM)	1.94 ± 0.29	1.53 ± 0.13	0.00 (–0.27 ± 0.22)
Ritonavir[c] (0.1 μM)	3.49 ± 0.44	12.0 ± 1.01	0.71 ± 0.11
Saquinavir[c] (20 μM)	13.7 ± 1.06	28.7 ± 1.41	0.52 ± 0.07
Talinolol (20 μM)	2.79 ± 0.27	3.53 ± 0.06	0.21 ± 0.18
Taxol[c] (10 μM)	2.05 ± 0.27	5.05 ± 0.88	0.59 ± 0.21
Verapamil (0.1 μM)	28.6 ± 2.30	49.2 ± 2.05	0.42 ± 0.07
Vinblastine (0.1 μM)	1.96 ± 0.20	7.62 ± 0.27	0.74 ± 0.08

[a] $P_{app,AB}$ values represent the mean of no less than three determinations ± SD.
[b] P_{PD} values represent the average of no less than three determinations performed in absorptive and secretory directions, respectively, ± SD. P_{PD} values in absorptive and secretory directions were not significantly different at $\alpha = 0.1$, except were noted.
[c] P_{PD} values determined in absorptive and secretory directions were significantly different ($a < 0.1$), and P_{PD} determined in absorptive direction are shown. P_{PD} values are reported as the mean of no less than three determinations ± SD.

Table IV. $P_{app,BA}$ and SQ Values Generated for P-glycoprotein Substrates in MDCK, Caco-2, and MDR-MDCK Cell Monolayers

	$P_{app,BA}$[a] (cm/s) × 10^6			SQ[b]		
Substrate (μM)	MDCK	Caco-2	MDR-MDCK	MDCK	Caco-2	MDR-MDCK
Acebutolol (20 μM)	7.82 ± 0.83	18.4 ± 0.24	17.2 ± 1.6	1.8 ± 0.37	1.9 ± 0.37	3.6 ± 0.46
Colchicine (25 μM)	5.44 ± 0.17	16.9 ± 0.60	11.9 ± 0.63	3.0 ± 0.73	5.1 ± 1.0	6.3 ± 0.72
Cyclosporin A[c] (0.1 μM)	14.9 ± 0.74	17.3 ± 1.1	9.70 ± 1.1	0.69 ± 0.13	1.5 ± 0.26	1.3 ± 0.62
Digoxin (10 μM)	17.1 ± 0.82	44.1 ± 0.85	35.7 ± 1.0	3.9 ± 0.53	2.0 ± 0.15	3.8 ± 0.20
Doxorubicin (10 μM)	4.60 ± 0.13	15.1 ± 0.57	15.5 ± 0.60	3.0 ± 1.4	25.5 ± 7.9	17.8 ± 3.2
Etoposide[d] (25 μM)	4.12 ± 0.29	14.0 ± 0.90	10.4 ± 1.2	1.9 ± 0.31	9.0 ± 2.0	14.9 ± 3.9
Methylprednisolone (20 μM)	35.7 ± 2.0	82.1 ± 4.2	94.3 ± 3.6	1.1 ± 0.15	1.3 ± 0.17	2.3 ± 0.20
Morphine (1 μM)	Not Determined	21.7 ± 0.37	14.4 ± 0.13	Not Determined	0.29 ± 0.06	0.67 ± 0.20
Prednisolone (20 μM)	27.0 ± 0.94	86.7 ± 1.6	84.9 ± 1.9	1.5 ± 0.12	1.0 ± 0.09	1.7 ± 0.09
Quinidine (1 μM)	75.4 ± 5.4	109 ± 2.7	156 ± 11.4	0.18 ± 0.16	0.95 ± 0.06	3.9 ± 0.60
Ranitidine (100 μM)	Not Determined	4.42 ± 0.36	3.29 ± 0.42	Not Determined	0.56 ± 0.36	1.6 ± 0.55
Rhodamine 123 (10 μM)	7.52 ± 0.28	16.2 ± 1.6	15.3 ± 4.1	3.9 ± 0.90	8.4 ± 2.1	5.8 ± 1.8
Ritonavir[c,e] (0.1 μM)	25.3 ± 4.5	40.4 ± 2.4	23.6 ± 2.2	0.40 ± 0.27	3.3 ± 0.42	2.7 ± 0.46
Saquinavir[c,e] (20 μM)	26.0 ± 0.39	80.3 ± 3.2	108 ± 3.4	0.35 ± 0.03	3.4 ± 0.29	5.1 ± 0.53
Talinolol[d] (20 μM)	9.71 ± 0.89	28.5 ± 0.12	22.8 ± 0.63	1.7 ± 0.29	2.5 ± 0.22	7.5 ± 0.56
Taxol[c–e] (10 μM)	35.7 ± 2.2	74.1 ± 2.1	62.9 ± 2.1	0.88 ± 0.12	1.2 ± 0.08	0.92 ± 0.10
Verapamil (0.1 μM)	55.9 ± 0.54	117 ± 1.2	93.2 ± 2.7	0.14 ± 0.04	0.36 ± 0.05	1.7 ± 0.13
Vinblastine[e] (0.1 μM)	9.92 ± 0.36	43.2 ± 1.5	35.7 ± 1.7	0.30 ± 0.06	1.4 ± 0.19	2.8 ± 0.30

[a] $P_{app,AB}$ values represent the mean of no less than three determinations ± SD.
[b] SQ values determined for MDCK, Caco-2, and MDR-MDCK monolayers were calculated using P_{PD} values listed in **Tables III, I,** and **II,** respectively (except when noted).
[c] P_{PD} ($n = 3$) determined in secretory direction in MDCK monolayers for cyclosporin-A (8.81 ± 0.69), ritonavir (18.10 ± 1.71), saquinavir (19.30 ± 0.29), and taxol (19.00 ± 0.39) were used to determine respective SQ.
[d] P_{PD} ($n = 3$) determined in secretory direction in Caco-2 monolayers for etoposide (1.40 ± 0.30), talinolol (8.51 ± 0.69), and taxol (33.10 ± 1.12) were used to determine respective SQ.
[e] P_{PD} ($n = 3$) determined in secretory direction in MDR-MDCK monolayers for ritonavir (6.44 ± 0.70), saquinavir (17.8 ± 1.71), taxol (32.7 ± 1.81), and vinblastine (9.44 ± 0.79) were used to determine respective SQ.

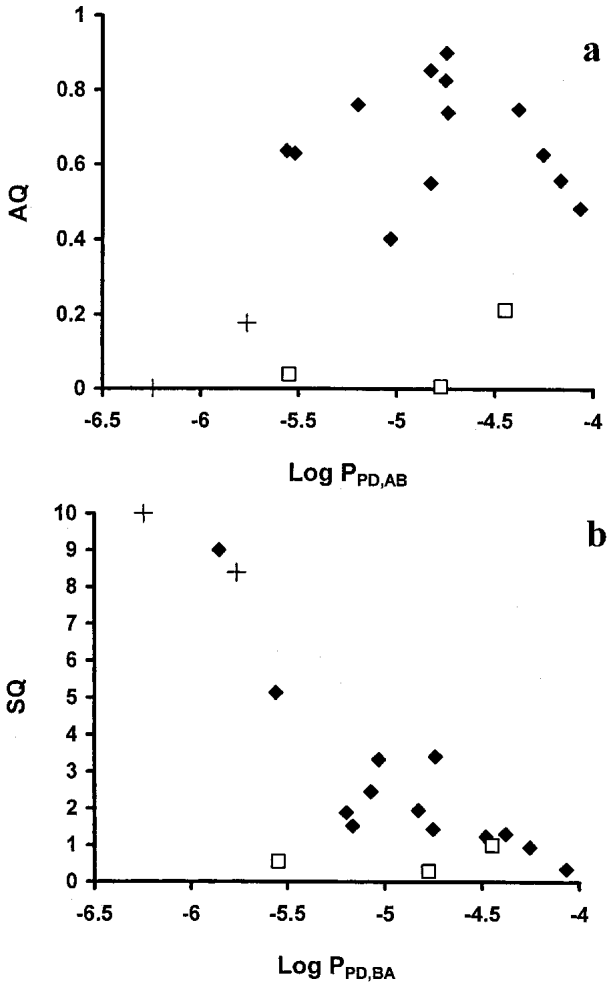

Fig. 2. AQ vs. Log $P_{PD,AB}$ (a) and SQ vs. Log $P_{PD,BA}$ (b), determined in Caco-2 Cell monolayers. ♦, Substrates with AQ ≥ 0.5 (class I); +, substrates with $AQ_{P\text{-}gp}$ < 0.3 and SQ > 2.0 (class II); □, substrates with AQ < 0.3 and SQ < 2.0 (class III).

Parameters to Assess Modulation of Transport by P-gp, AQ and SQ vs. Efflux Ratio

The parameters to assess attenuation of absorptive transport (AQ) and enhancement of secretory transport (SQ) in the three cell culture models were derived from the respective apparent permeability values ($P_{app,AB}$ and $P_{app,BA}$) and the permeability due to passive diffusion (P_{PD}; Tables I-IV). The AQ values spanned a wide range, from 0 to 0.9, with a theoretical range of 0 to 1. The absorptive transport of doxorubicin, rhodamine 123, morphine, prednisolone, and ranitidine was not much affected by P-gp-mediated efflux activity in Caco-2 cells (AQ < 0.2). P-gp attenuated the absorptive transport of the remainder of the substrates (by at least 50%), as evidenced by their AQ values (0.5 ≤ AQ ≤ 0.9). The behavior of compounds with respect to their AQ values in the MDR-MDCK cells were similar to that in the Caco-2 cells. In general, the AQ values were smaller in MDCK cell monolayers than in Caco-2 or MDCK-MDR cell monolayers. This is consistent with lower expression of P-gp in MDCK cells in comparison to the other two cell culture systems (45,46). However, it is interesting to note that absorptive transport of several compounds was significantly attenuated in MDCK cells as evidenced by AQ values of greater than 0.5. In all three cell culture models, the maximal AQ values were observed for moderately permeable substrates (P_{PD} approx. 5-15 × 10^{-6} cm/s).

Interestingly, the SQ values of the compounds were not directly related to their AQ values. For example, the minimally permeable doxorubicin and rhodamine 123 showed very low AQ values but large SQ values in each cell line. Generally, substrates with lower P_{PD} values (e.g. doxorubicin, rhodamine 123, etoposide, and colchicine) had the greatest SQ values in each cell model. SQ values were greater in Caco-2 and MDR-MDCK vs. MDCK cell monolayers (except digoxin). Although AQ values observed in Caco-2 and MDR-MDCK monolayers were nearly identical, increases in SQ were observed for most substrates in MDR-MDCK vs. Caco-2 cell monolayers; only SQ values of doxorubicin, rhodamine 123, taxol, ritonavir and cyclosporin-A were less or equal in MDR-MDCK vs. Caco-2 cells.

Comparison of AQ values that directly quantified how P-gp attenuates absorptive transport, with the respective efflux ratios that measured (apically-directed) transport polarity, revealed several discrepancies (Table I). The following examples highlight where information provided by AQ values and efflux ratios (with regards to the functional activity of P-gp during absorptive transport) differs. Although P-gp does not affect the absorptive transport of rhodamine 123 or doxorubicin, the efflux ratios of these substrates are large. The AQ values of acebutolol, methylprednisolone, and saquinavir are nearly equal—showing P-gp equally affects the absorptive transport of these compounds—but the efflux ratios of these substrates are very different. Although the efflux ratios of cyclosporin-A, talinolol, verapamil, and quinidine were among the lowest observed, the AQ values determined for these substrates show that P-gp-mediated efflux activity highly reduces their absorptive transport across Caco-2 cell monolayers. AQ values and efflux ratios were in reasonable agreement (with respect to rank order of magnitude) for morphine, ranitidine, prednisolone, and taxol.

Relationship of AQ and SQ to P_{PD} and P-gp Expression

Figure 2 is a representative plot of AQ and SQ vs. P_{PD} values in Caco-2 cell monolayers (a qualitatively similar profile was observed in MDR-MDCK cells). AQ and SQ are related to P_{PD} in very different ways. In contrast to AQ, SQ appeared to decay exponentially as log P_{PD} increased. Substrates such as rhodamine 123 and doxorubicin with low AQ, but high SQ, and substrates such as morphine, ranitidine, and prednisolone with low AQ and SQ showed no relationship between AQ and P_{PD}. Substrates with "high" AQ values (~ ≥ 0.5) displayed a trend for parabolic relationship with AQ, although there was some scatter in the data (two outliers); AQ increased as P_{PD} was increased to a maximal value of P_{PD} approx. 7 to 20 × 10^{-6} cm/s, and then decreasing with further increases in P_{PD}. Whereas cyclosporin-A and ritonavir did not strictly obey the parabolic relationship in Caco-2 cells, only ritonavir did not obey the relationship in MDR-MDCK cells. Furthermore, as P-gp expression was decreased (from MDR-MDCK to Caco-2 to MDCK), the parabolic relationship became more scattered; thus AQ values of cyclosporin A, colchicine, acebutolol, talinolol, methylpredniso-

Table V. $P_{app,AB}$, and AQ Values for P-glycoprotein Substrates Generated in MDR-MDCK Cell Monolayers in the Presence of 45 and 85 nM GW918

Substrate (μM)	$P_{aap,AB}$[a] (cm/s) × 10^6		AQ[b]	
	+45 nM GW918	+85 nM GW918	+45 nM GW918	+85 nM GW918
Acebutolol (20 μM)	2.00 ± 0.45	2.63 ± 0.16	0.46 ± 0.14	0.29 ± 0.08
Colchicine (25 μM)	0.92 ± 0.17	1.19 ± 0.14	0.44 ± 0.20	0.27 ± 0.19
Cyclosporin A (0.1 μM)	2.64 ± 0.14	3.51 ± 0.34	0.39 ± 0.15	0.19 ± 0.16
Digoxin (10 μM)	3.47 ± 0.83	5.10 ± 0.84	0.54 ± 0.15	0.32 ± 0.15
Etoposide (25 μM)	0.34 ± 0.11	0.43 ± 0.01	0.48 ± 0.24	0.34 ± 0.16
Methylprednisolone (20 μM)	13.4 ± 0.82	18.3 ± 0.19	0.53 ± 0.18	0.36 ± 0.17
Prednisolone (20 μM)	18.1 ± 4.83	22.8 ± 7.60	0.34 ± 0.18	0.16 ± 0.28
Quinidine (1 μM)	13.3 ± 2.9	18.6 ± 0.93	0.58 ± 0.10	0.41 ± 0.04
Ritonavir (0.1 μM)	2.51 ± 0.52	3.11 ± 0.60	0.36 ± 0.15	0.21 ± 0.17
Saquinavir (20 μM)	3.26 ± 0.66	5.39 ± 0.34	0.74 ± 0.50	0.57 ± 0.46
Talinolol (20 μM)	1.66 ± 0.28	2.28 ± 0.07	0.38 ± 0.15	0.15 ± 0.10
Taxol (10 μM)	2.40 ± 0.26	2.65 ± 0.23	0.67 ± 0.11	0.64 ± 0.11
Verapamil (0.1 μM)	20.0 ± 1.45	23.4 ± 2.33	0.43 ± 0.06	0.33 ± 0.08
Vinblastine (0.1 μM)	0.80 ± 0.15	1.19 ± 0.18	0.82 ± 0.22	0.73 ± 0.21

[a] $P_{app,AB}$ values represent the mean of no less than three determinations ± SD.
[b] AQ values were calculated using MDR-MDCK P_{PD} values shown in Table II.

lone, and prednisolone showed no relationship to P_{PD} in MDCK monolayers.

Although P-gp expression was approximately 1.5-fold greater in MDR-MDCK vs. Caco-2 monolayers, the AQ values obtained in these two cell culture models were nearly identical (exceptions: prednisolone, cyclosporin A, and talinolol). This finding may suggest that the functional activity of P-gp that is manifested during absorptive transport is maximal at an expression level comparable to that observed in Caco-2 monolayers for most P-gp substrates. As expected, most AQ values were significantly lower in MDCK cell monolayers than in Caco-2 or MDR-MDCK cell monolayers (Tables I–III). Curiously, AQ determined for ritonavir in MDCK monolayers was greater than that determined in Caco-2 or MDR-MDCK monolayers. The AQ values of vinblastine, etoposide, taxol, verapamil, etoposide, quinidine, and digoxin in MDCK cell monolayers were very comparable with those in Caco-2 and MDR-MDCK cell monolayers (<1.7-fold difference in AQ values in MDCK vs. Caco-2 or MDR-MDCK cell monolayers), despite the large differences in P-gp expression observed between these cell models. For acebutolol, colchicine, cyclosporin-A, methylprednisolone, prednisolone, and talinolol, AQ values in MDCK monolayers were 2.5-fold less than those in Caco-2 (except prednisolone) or MDR-MDCK monolayers. These results suggest that attenuation of absorptive transport for some compounds may be much less dependent on the level of P-gp expression than for other compounds. The magnitude of SQ per given P_{PD} generally increased with increasing protein expression.

Table VI. IC_{50} (AQ) Determined in MDR-MDCK Cell Monolayers

Substrate (μM)	IC_{50} (AQ) (nM)[a]
Vinblastine (0.1 μM)	>100
Taxol (10 μM)	>100
Verapamil (0.1 μM)	>100
Saquinavir (20 μM)	>100
Etoposide (25 μM)	>100
Quinidine (1 μM)	>100
Methylprednisolone (20 μM)	83.4 ± 14.7
Colchicine (25 μM)	83.2 ± 27.2
Digoxin (10 μM)	80.2 ± 28.8
Ritonavir (0.1 μM)	72.9 ± 24.4
Prednisolone (20 μM)	70.0 ± 41.0
Acebutolol (20 μM)	48.5 ± 5.26
Talinolol (20 μM)	35.5 ± 14.7
Cyclosporin A (0.1 μM)	32.0 ± 7.48

[a] IC_{50} (AQ) value is the concentration of GW918 that caused a 50% reduction in AQ_{max} (determined under normal conditions) ± standard error.

Titration of P-gp in MDR-MDCK Cells with GW918: An Alternative Approach to Investigate the Relationship between Functional Activity of P-gp and Absorptive Transport

Performing studies with Caco-2, MDR-MDCK, and MDCK cell monolayers provided some insight into the relationship between substrate P_{PD} and the functional activity of P-gp. However, confounding cell model-dependent differences made it difficult to elucidate the complex relationship of P-gp expression, substrate P_{PD}, and interaction of the substrate with P-gp to the functional activity of P-gp. To clearly elucidate this relationship, an experimental strategy was conceived that simulated P-gp expression changes without altering substrate P_{PD} or interaction with P-gp. By using the noncompetitive P-gp inhibitor GW918 (37,44) at 45 and 85 nM, concentrations that reduced MDR-MDCK AQ for digoxin by approx. 40 and 70%, respectively (preliminary experiments, and Table V)—it was possible to systematically reduce Jmax for P-gp-mediated efflux activity, analogous to reducing P-gp expression.

The absorptive P_{app} values and AQ values in MDR-MDCK cells treated with 45 nM and 85 nM GW918 are shown in Table V. The IC_{50} (AQ) was determined (see Theory section) to provide a measure of how substrate AQ decreased in response to decreases in apparent P-gp expres-

Table VII. Substrate Classification for Patterns of P-Glycoprotein (P-gp) Functional Activity Observed Using *in Vitro* Models of Polarized Epithelium with P-gp Expression Level Comparable to Normal Human Intestine[a]

	I[c]			
Class subclass[b]	High responders	Low responders	II[d]	III[e]
	Acebutolol	Etoposide	Doxorubicin	Morphine
	Colchicine	Quinidine	Rhodamine 123	Ranitidine
	Cyclosporin A	Saquinavir		
	Digoxin	Taxol		
	Methylprednisolone	Verapamil		
	Prednisolone[f]	Vinblastine		
	Ritonavir			
	Talinolol			

[a] Caco-2 and MDR-MDCK cell monolayers have P-gp expression level comparable with normal human intestine.
[b] Subclass is based on how AQ changes in response to changes in P-gp expression (J_{max}). Criteria for subclasses are based on IC_{50} (AQ) for functional activity of P-gp determined in MDR-MDCK cell monolayers. Those substrates with "low" IC_{50} (AQ) values <100 nM) were placed in subclass high responders. Those substrates with "high" IC_{50} (AQ) values (>100 nM) were placed in subclass low responders.
[c] Criteria for Class I is AQ $\geq$ 0.5.
[d] Criteria for Class II is AQ < 0.5 and SQ $\geq$ 2.0.
[e] Criteria for Class III is AQ < 0.5 and SQ < 2.0.
[f] Prednisolone is an ambiguous Class I substrate.

sion (J_{max}) achieved by addition of GW918 (Table VI). Interestingly, the IC_{50} (AQ) values determined for these substrates could be grouped into two categories. The AQ values for vinblastine, taxol, etoposide, quinidine, saquinavir, and verapamil changed very little in the presence of 45 and 85 nM GW918 (estimated IC_{50} [AQ] >100 nM), and were designated as low responders. In contrast, the AQ values of ritonavir, digoxin, methylprednisolone, prednisolone, and colchicine (mean IC_{50} [AQ] = 77.9 ± 6.14 nM) as well as of acebutolol, talinolol, and cyclosporin A (mean IC_{50} [AQ] = 38.7 ± 8.69) decreased rapidly with increasing GW918 concentrations, and hence were designated as high responders.

DISCUSSION

The presence of the apically directed efflux pump, P-gp, in the intestinal epithelium can potentially lead to a reduction in the absorption of its substrates. In cell monolayers used as models for intestinal epithelium, P-gp causes a polarized transport of its substrates such that the secretory flux is much greater than the absorptive flux. Frequently, the magnitude of the ratio of secretory vs. absorptive flux (efflux ratio) is construed as the potential effect of P-gp on absorption, with an implicit assumption that the effect of P-gp on absorptive and secretory transport is symmetric. This study was initiated because of our recent observation that the effect of P-gp in attenuating absorptive transport and enhancing secretory transport is asymmetric (31), and thus efflux ratios do not always provide a good estimate of the attenuation of intestinal absorption of compounds by P-gp.

AQ and SQ

We propose that the effect of P-gp on absorptive transport alone, without comparison of the effect of P-gp on the secretory transport, be used to assess the potential effect of this efflux pump on intestinal absorption. Similarly, only the effect of P-gp on the secretory transport should be used to assess the effect of P-gp on intestinal secretion. To accomplish this, we propose that the absorptive (or secretory) flux be measured under the normal cell culture condition (with fully functional P-gp) and after complete inhibition of P-gp with a selective P-gp inhibitor, such as the non-competitive P-gp inhibitor, GW918. The effect of P-gp on the attenuation of absorptive (and enhancement of secretory) transport can be quantified from these experimental results, and expressed conveniently as the novel parameter AQ (and SQ). AQ and SQ provide unambiguous information on the extent to which P-gp affects absorptive (using AQ) or secretory (using SQ) transport of a substrate across polarized epithelium (Tables I–IV). It is important to recognize that AQ and SQ are not subject to the influences of other transport processes and differences in transport pathways that can confound measures of apically-directed transport polarity (i.e. efflux ratio) (30,31). A clear advantage of these parameters is that they quantify the functional activity of P-gp in a way that clearly shows how P-gp-mediated efflux activity affects transport across polarized epithelium (e.g., AQ = 0.5 indicates that P-gp attenuates transport by 50%). Further, AQ and SQ can be determined individually; so if one wants information on the effect of P-gp on just absorptive transport, only AQ need to be determined. Generation of AQ and SQ represents an efficient experimental approach to 1) positively identify P-gp substrates in polarized epithelium, 2) quantify the functional effect of P-gp on absorption and secretion, and 3) determine (or approximate) the passive diffusion component (P_{PD}) of the transport of the compound.

Determinants of the Functional Activity of P-gp

For a P-gp substrate, P_{PD} (i.e., passive diffusivity) and parameters that define its interaction with P-gp (i.e., K_m and maximal efflux; J_{max}) are critical determinants of the modu-

lation of its absorptive and/or secretory transport caused by P-gp during substrate transport across polarized epithelium (40,43,47–49). In addition, the level of P-gp expression is also a critical determinant of the functional activity of P-gp (40,43,47–49). To assess how changes in these determinants affect the functional activity of P-gp, substrates from diverse chemical classes that spanned a wide range of drug P_{PD} across polarized epithelium were selected (see Table I). It was expected that the variety in chemical structures would provide sufficient variability in substrate interactions with P-gp. Further, studies were performed with the P-gp substrate set in the *in vitro* models of polarized epithelium, Caco-2, MDR-MDCK, and MDCK cell monolayers, in order to explore how changes in the level of P-gp expression, in addition to substrate P_{PD} and interaction with P-gp, affect the functional activity of P-gp during substrate transport across intestinal epithelium (Tables I–IV). These *in vitro* models were selected based on reports of P-gp expression differences observed for these cell lines (greatest in MDR-MDCK and least in MDCK monolayers) (45,46). Indeed, our own results agreed with these reports, and showed that the P-gp expression level was an order of magnitude lower in MDCK cells than in Caco-2 cells. Interestingly, the level of P-gp expression was only slightly lower in Caco-2 cells than in MDR-MDCK cells. Western blot analysis also revealed that the level of P-gp expression in Caco-2 and MDR-MDCK monolayers is comparable to that of the normal human intestine (Fig. 1).

Relative Merits of AQ vs. Efflux Ratio as a Tool To Assess How P-gp Attenuates Absorption

Table I compares the AQ values and efflux ratios for 18 P-gp substrates, determined in Caco-2 cells. These compounds exhibit a wide range of $P_{app,AB}$ and P_{PD} values. Out of these 18 compounds, the efflux ratio is > 40 for 1 compound, between 20–40 for 2 compounds, between 10–20 for six compounds, between 5–10 for four compounds, and <5 for five compounds. These values do not reveal how P-gp is affecting the absorptive transport of any of these compounds. In contrast, the AQ values clearly reveal the percentage by which P-gp attenuates the absorptive transport of these compounds in the same Caco-2 cell culture model. Thus P-gp attenuates the absorptive transport of three compounds by less than 10%, of four compounds by 10 to 50%, and of the remaining 11 compounds by >50%. Clearly, the AQ values are much more meaningful in assessing the potential of P-gp in attenuating absorption of these compounds. It is interesting to note that for compounds like doxorubicin, the efflux ratio is >25, and yet the AQ value is 0. Such comparison reveals that a large efflux ratio may falsely predict a large P-gp effect on oral absorption of doxorubicin. In contrast, doxorubicin does exhibit a large value of SQ (Table IV), suggesting that P-gp contributes very significantly to enhancement of the secretory transport of doxorubicin, thus explaining the large value of the efflux ratio. Prednisolone and methylprednisolone provide another example of how AQ values are much more predictive than efflux ratios of P-gp's role in absorptive transport. The efflux ratios for prednisolone and methylprednisolone are 3.4 and 7.8, respectively, indicative of modest effect of P-gp in their absorptive transport. However, the respective AQ values of 0.21 and 0.75 for the two compounds suggest that absorption of methylprednisolone should be much more affected by P-gp than that of prednisolone. Interestingly, the *in vivo* data in rats clearly show that absorption of methylpredenisolone is attenuated by P-gp, whereas the absorption of prednisolone is not (9).

Substrate Classification of How P-gp Affects Transport Using AQ and SQ Values

Based on the values of AQ and SQ obtained in Caco-2 cells and MDR-MDCK cells, both expressing levels of P-gp within the range found in human intestinal epithelium (Fig. 1), the compounds are classified into three classes (Table VII). Class I includes substrates whose absorptive transport is highly attenuated by P-gp-mediated efflux activity. The criterion for 'high' attenuation is AQ $\geq$ 0.5. Class II substrates are hydrophilic cations, e.g., rhodamine 123 and doxorubicin, with secretory, but not absorptive, transport highly affected by P-gp-mediated efflux activity (30). The criterion for "high" enhancement of secretory transport is SQ $\geq$ 2.0, and for "low" attenuation of absorptive transport is AQ < 0.5. The class II compounds primarily use the paracellular pathway during absorptive transport (thus, P-gp cannot affect absorptive transport), but use the transcellular pathway during secretory transport, presumably due to carrier-mediated uptake across the BL membrane (P-gp-mediated efflux activity then plays a major role in export of the membrane-impermeable compound across AP membrane). Finally, Class III is composed of compounds that are not highly affected by P-gp-mediated efflux activity in either transport direction. It was observed that for the class III substrates, morphine and ranitidine, the AQ and SQ values determined in Caco-2 and MDR-MDCK monolayers were much less than 0.5 and 2.0, respectively. Classification of only one substrate, prednisolone, was ambiguous. In Caco-2 monolayers, this compound would be a class III substrate; however, in MDR-MDCK monolayers, prednisolone would be tentatively placed in class I. The good agreement of substrate classification in Caco-2 and MDR-MDCK monolayers suggests that these two *in vitro* models can be used interchangeably to assess the functional effect of P-gp on drug absorption or secretion.

Relationships of the Functional Activity of P-gp (during Absorptive Transport) to P_{PD}, Protein Expression, and Kinetic Parameters of P-gp Substrates

The use of Caco-2, MDR-MDCK, and MDCK cells provided some insights into the changes in AQ values with gross changes in expression level of P-gp. However, in order to examine the interrelationship among the key determinants of P-gp-mediated attenuation of absorptive transport (AQ), it was necessary to achieve graded changes in P-gp expression level while simultaneously keeping interaction of the compound with P-gp and the passive diffusivity properties of each compound constant. We have accomplished this by titrating down P-gp-mediated efflux activity with the noncompetitive P-gp inhibitor GW918 (37,44) to simulate changes in P-gp expression. Presumably, J_{max} (but not K_m) for P-gp-mediated efflux activity is altered by changes in expression, or in the presence of a non-competitive inhibitor. MDR-MDCK monolayers were used in this approach due to their short culture time, and because the data suggest that maximal functional activity of P-gp occurs at a level of P-gp expression observed in Caco-2 or MDR-MDCK monolayers (Fig. 1 and

Table II). It is assumed in this experimental approach that GW918 has no effect on substrate interaction with P-gp (44), and on substrate P_{PD} across polarized epithelium. To quantify the changes in functional activity of P-gp toward different substrates with changes in Jmax, the concentration of GW918 that caused 50% reduction in AQ with respect to the control value (IC_{50} [AQ], Table VI) was determined. These values showed an inverse relationship with reported K_d values (44,50–53). It was not intended for this IC_{50} (AQ) to quantify substrate binding affinity to P-gp; instead, this value was used as a guide in understanding how changes in J_{max} affect the functional activity of P-gp during the absorptive transport of the substrate (it is however reasonable, based on Michaelis-Menten kinetics, that under certain conditions this IC_{50} (AQ) could be used a surrogate measure of substrate binding to P-gp). As expected, the AQ of the 14 class I substrates included in this study decreased as P-gp was inhibited with increasing concentrations of GW918 (decreases in apparent J_{max}). However, the AQ was not equally sensitive to changes in P-gp activity (apparent J_{max}) for all substrates as evidenced by different IC_{50} (AQ) values observed (Table VI). In fact, based on the IC_{50} (AQ) values, we have classified the compounds as high responders (IC_{50} [AQ] < 100 nM) and low responders (IC_{50} [AQ] > 100 nM) (Table VII).

When AQ values of high and low responders, determined in MDR-MDCK cells at different apparent J_{max} of P-gp, are plotted against log P_{PD} (Fig. 3), it becomes apparent that these two groups of compounds also behave differently to changes in P_{PD}. Regardless of the level of P-gp activity, the AQ values of low responders exhibit an approximate parabolic relationship with log P_{PD} (Fig. 3a), whereas those of the high responders are generally unaffected by changes in P_{PD} (Fig. 3b). Fig. 3 graphically demonstrates that for compounds with wide range of P_{PD} values, the AQ values of low responders change much less than those of the high responders as the P-gp activity is altered by inhibition with GW918. This observed parabolic relationship of the functional activity of P-gp to P_{PD} during absorptive transport of low responders is in agreement with published reports, which used a kinetic model to show that substrates with moderate P_{PD} are affected by P-gp to a greater extent than those with high or low P_{PD} (27,43). However, what has not been recognized previously is the fact that for certain groups of compounds (identified here as high responders), the absorptive transport affected by P-gp is not primarily dependent on their passive diffusivity (P_{PD}). Re-evaluation of the AQ values determined for the low responders in Caco-2 and MDCK monolayers displayed similar parabolic relationships with log P_{PD} as those observed in MDR-MDCK monolayers. Although P-gp expression in Caco-2 and MDR-MDCK monolayers is 9- and 13-fold greater than that in MDCK monolayers, respectively, the magnitude of the AQ of the low responders was increased only slightly to moderately (< 1.7-fold) in Caco-2 or MDR-MDCK vs. MDCK cell monolayers. Conversely, the AQ values of the high responders increased in Caco-2 and MDR-MDCK vs. MDCK monolayers by significantly greater than 2-fold (except ritonavir and prednisolone). The AQ values of these high responders were independent of P_{PD} in all three cell culture models that exhibited a wide range of P-gp expression. These results are entirely consistent with the results in Fig. 3b, which showed a similar lack of relationship between AQ and passive diffusivity in MDR-MDCK cells at

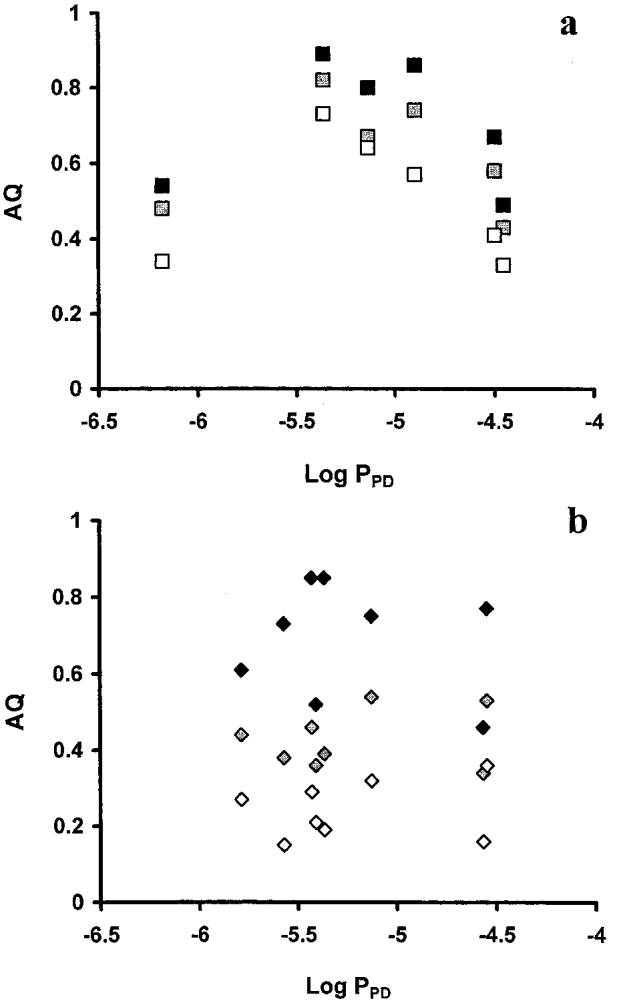

Fig. 3. $AQ_{P\text{-}gp}$ Values for class I low responders (a) and high responders (b) vs. Log P_{PD}. Data are shown for cells titrated to different J_{max} of P-gp-mediated efflux activity. To achieve this, AQ values were determined in MDR-MDCK monolayers under normal conditions (black symbols) and in the presence of 45 nM and 85 nM GW918 (gray and white symbols, respectively) vs. Log P_{PD}.

three widely varying levels of P-gp activity. Thus, the data generated in Caco-2, MDCK, and MDR-MDCK monolayers were in good agreement with data generated using the GW918 titration method in MDR-MDCK monolayers with regards to the role of P-gp expression (J_{max}) and P_{PD} in defining the functional activity of P-gp during absorptive transport of compounds across polarized epithelium. This leads us to conclude that the GW918 titration method is a viable experimental approach to simulate P-gp expression level changes in polarized epithelium, and that this approach can be used to determine how P-gp substrates would behave with respect to different P-gp expression and varying passive diffusivity.

Relationship of the Functional Activity of P-gp (during Secretory Transport) to P_{PD} and Protein Expression

Finally, the relationship of P-gp expression and substrate P_{PD} to the functional activity of P-gp during secretory transport was briefly explored. In MDCK, Caco-2, and MDR-MDCK monolayers, SQ of class I and II substrates (see Table

IV for SQ values) generally decreases with increasing log P_{PD} in an exponential fashion (shown for Caco-2 cells in Fig. 2). Although class II SQ values decreased with increasing P_{PD}, this finding must be interpreted with caution because of the limited number of class II substrates included in these studies, and because these class II substrates are substrates for uptake carriers located on the BL membrane (30). Interestingly, the SQ values for all class I substrates appear to be highly dependent on both substrate P_{PD} and P-gp expression level. In each cell type, SQ decreases sharply with increasing P_{PD} up to P_{PD} of approx. 5×10^{-6} cm/s, and then gradually with further increases in P_{PD} (data only plotted for Caco-2 cells, Fig. 2). Increases in SQ for all class I substrates were observed in Caco-2 vs. MDCK monolayers (except digoxin), and in MDR-MDCK vs. Caco-2 monolayers (except taxol and ritonavir). It is noteworthy that whereas AQ (for class I substrates) is generally maximal at a protein expression level comparable to that of Caco-2 monolayers, SQ values were not maximized at the expression levels observed in these studies.

CONCLUSIONS

These observations about the relationship of AQ and SQ to P-gp expression level and passive diffusivity clearly support our hypothesis that the effect of P-gp on the absorptive and secretory transport is asymmetric, perhaps due to 1) different absorptive and secretory transport mechanisms of certain compounds and/or 2) different barrier properties (lipid composition) of the AP vs. BL membrane in polarized epithelia (54–58) . Therefore, we strongly recommend that the use of parameters that only describe the overall polarity of transport due to P-gp (i.e., efflux ratio) should be avoided to assess the effect of P-gp on intestinal drug absorption. Instead, we recommend the use of parameters, such as AQ and SQ, which can independently quantify the effect of P-gp on absorptive and secretory transport, respectively. Of course, for those who are only interested in the effect of P-gp on intestinal absorption, only AQ needs to be determined. Our analysis of changes in AQ with changes in passive diffusivity of compounds and P-gp expression level has revealed that the effect of P-gp on attenuating absorptive transport of compounds is quite complex. Thus, the previously held belief that P-gp would be less effective in attenuating absorption of compounds with greater passive diffusion coefficients is not true for all compounds. Even more refined proposals involving parabolic relationship between attenuation of transport by P-gp and passive diffusion permeability are not necessarily true for all compounds. Similarly, the relationship between attenuation of transport by P-gp and the level of P-gp expression is different for different sets of compounds. In addition to highlighting the complexity of these relationships, we have developed some experimental approaches to classify compounds based on their absorptive and secretory behavior as they interact with P-gp (Table VII). Admittedly, the classification is based on a rather limited set of compounds, but it does provide valuable insights on differential absorptive behavior of compounds when they interact with P-gp during transport across polarized epithelia.

ACKNOWLEDGMENTS

Financial support for this research was provided by a fellowship from the PhRMA Foundation and by grants from DuPont Pharmaceuticals Company and Parke-Davis. The authors would like to thank the following for their generous donations: Drs. Mary F. Paine and Paul B. Watkins, both of the University of North Carolina at Chapel Hill for providing Caco-2 cells and human intestinal homogenates; Dr. Piet Borst of The Netherlands Cancer Institute for providing MDR-MDCK cells; Dr. Moo J. Cho of the University of North Carolina at Chapel Hill for providing Cyclosporin A; Dr. Gary M. Pollack of the University of North Carolina at Chapel Hill for providing morphine, [^{3}H]-morphine, ritonavir, [^{3}H]-ritonavir [^{3}H]-verapamil, and [^{3}H]-vinblastine; Dr. Ken Brouwer and GlaxoSmithKline for providing GW918; Arzneimittelwerk Dresden GmbH for providing talinolol; and Roche Discovery Welwyn for providing saquinavir. The authors would like to especially thank Dr. Mary F. Paine for her helpful discussions and her expert advice regarding Western blot analysis of P-gp. The authors would like to thank Drs. Ronald T. Borchardt and Fuxing Tang of The University of Kansas, Lawrence, KA, for their advice in MDR-MDCK cell culture.

REFERENCES

1. F. Thiebaut, T. Tsuruo, H. Hamada, M. M. Gottesman, I. Pastan, and M. C. Willingham. Cellular localization of the multidrug-resistance gene product P- glycoprotein in normal human tissues. *Proc. Natl. Acad. Sci. USA* **84**:7735–7738 (1987).
2. J. Hunter, B. H. Hirst, and N. L. Simmons. Drug absorption limited by P-glycoprotein-mediated secretory drug transport in human intestinal epithelial Caco-2 cell layers. *Pharm. Res.* **10**: 743–749 (1993).
3. P. F. Augustijns, T. P. Bradshaw, L. S. Gan, R. W. Hendren, and D. R. Thakker. Evidence for a polarized efflux system in CACO-2 cells capable of modulating cyclosporin A transport. *Biochem. Biophys. Res. Commun.* **197**:360–365 (1993).
4. T. Gramatte, R. Oertel, B. Terhaag, and W. Kirch. Direct demonstration of small intestinal secretion and site-dependent absorption of the beta-blocker talinolol in humans. *Clin. Pharmacol. Ther.* **59**:541–549 (1996).
5. M. F. Hebert. Contributions of hepatic and intestinal metabolism and P-glycoprotein to cyclosporine and tacrolimus oral drug delivery. *Adv. Drug Deliv. Rev.* **27**:201–214 (1997).
6. W. M. Kan, Y. T. Liu, C. L. Hsiao, C. Y. Shieh, J. H. Kuo, J. D. Huang, and S. F. Su. Effect of hydroxyzine on the transport of etoposide in rat small intestine. *Anticancer Drugs* **12**:267–273 (2001).
7. M. Sababi, O. Borga, and U. Hultkvist-Bengtsson. The role of P-glycoprotein in limiting intestinal regional absorption of digoxin in rats. *Eur. J. Pharm. Sci.* **14**:21–27 (2001).
8. H. Saitoh and B. J. Aungst. Possible involvement of multiple P-glycoprotein-mediated efflux systems in the transport of verapamil and other organic cations across rat intestine. *Pharm. Res.* **12**:1304–1310 (1995).
9. H. Saitoh, M. Hatakeyama, O. Eguchi, M. Oda, and M. Takada. Involvement of intestinal P-glycoprotein in the restricted absorption of methylprednisolone from rat small intestine. *J. Pharm. Sci.* **87**:73–75 (1998).
10. H. Spahn-Langguth, G. Baktir, A. Radschuweit, A. Okyar, B. Terhaag, P. Ader, A. Hanafy, and P. Langguth. P-glycoprotein transporters and the gastrointestinal tract: evaluation of the potential in vivo relevance of in vitro data employing talinolol as model compound. *Int. J. Clin. Pharmacol. Ther.* **36**:16–24 (1998).
11. A. Sparreboom, J. van Asperen, U. Mayer, A. H. Schinkel, J. W. Smit, D. K. Meijer, P. Borst, W. J. Nooijen, J. H. Beijnen, and O. van Tellingen. Limited oral bioavailability and active epithelial excretion of paclitaxel (Taxol) caused by P-glycoprotein in the intestine. *Proc. Natl. Acad. Sci. USA* **94**:2031–2035 (1997).
12. R. B. Kim, M. F. Fromm, C. Wandel, B. Leake, A. J. Wood, D. M. Roden, and G. R. Wilkinson. The drug transporter P-glycoprotein limits oral absorption and brain entry of HIV-1 protease inhibitors. *J. Clin. Invest.* **101**:289–294 (1998).

13. R. B. Kim, C. Wandel, B. Leake, M. Cvetkovic, M. F. Fromm, P. J. Dempsey, M. M. Roden, F. Belas, A. K. Chaudhary, D. M. Roden, A. J. Wood, and G. R. Wilkinson. Interrelationship between substrates and inhibitors of human CYP3A and P-glycoprotein. *Pharm. Res.* **16**:408–414 (1999).
14. W. L. Chiou, S. M. Chung, and T. C. Wu. Commentary: Potential role of P-glycoprotein in affecting hepatic metabolism of drugs. *Pharm. Res.* **17**:901–903 (2000).
15. K. Arimori and M. Nakano. Drug exsorption from blood into the gastrointestinal tract. *Pharm. Res.* **15**:371–376 (1998).
16. U. Mayer, E. Wagenaar, J. H. Beijnen, J. W. Smit, D. K. Meijer, J. van Asperen, P. Borst, and A. H. Schinkel. Substantial excretion of digoxin via the intestinal mucosa and prevention of long-term digoxin accumulation in the brain by the mdr 1a P-glycoprotein. *Br. J. Pharmacol.* **119**:1038–1044 (1996).
17. T. Gramatte and R. Oertel. Intestinal secretion of intravenous talinolol is inhibited by luminal R- verapamil. *Clin. Pharmacol. Ther.* **66**:239–245 (1999).
18. J. van Asperen, A. H. Schinkel, J. H. Beijnen, W. J. Nooijen, P. Borst, and O. van Tellingen. Altered pharmacokinetics of vinblastine in Mdr1a P-glycoprotein- deficient Mice. *J. Natl. Cancer Inst.* **88**:994–999 (1996).
19. J. van Asperen, O. van Tellingen, and J. H. Beijnen. The role of mdr1a P-glycoprotein in the biliary and intestinal secretion of doxorubicin and vinblastine in mice. *Drug Metab. Dispos.* **28**:264–267 (2000).
20. U. Wetterich, H. Spahn-Langguth, E. Mutschler, B. Terhaag, W. Rosch, and P. Langguth. Evidence for intestinal secretion as an additional clearance pathway of talinolol enantiomers: concentration- and dose-dependent absorption in vitro and in vivo. *Pharm. Res.* **13**:514–522 (1996).
21. S. Ito, C. Woodland, P. A. Harper, and G. Koren. P-glycoprotein-mediated renal tubular secretion of digoxin: the toxicological significance of the urine-blood barrier model. *Life Sci.* **53**:L25–L31 (1993).
22. A. Johne, J. Brockmoller, S. Bauer, A. Maurer, M. Langheinrich, and I. Roots. Pharmacokinetic interaction of digoxin with an herbal extract from St John's wort (Hypericum perforatum). *Clin. Pharmacol. Ther.* **66**:338–345 (1999).
23. B. Greiner, M. Eichelbaum, P. Fritz, H. P. Kreichgauer, O. von Richter, J. Zundler, and H. K. Kroemer. The role of intestinal P-glycoprotein in the interaction of digoxin and rifampin. *J. Clin. Invest.* **104**:147–153 (1999).
24. J. G. Theis, H. S. Chan, M. L. Greenberg, D. Malkin, V. Karaskov, I. Moncica, and G. Koren. and J. Doyle. Increased systemic toxicity of sarcoma chemotherapy due to combination with the P-glycoprotein inhibitor cyclosporin. *Int. J. Clin. Pharmacol. Ther.* **36**:61–64 (1998).
25. M. F. Paine, L. Y. Leung, H. K. Lim, K. Liao, A. Oganesian, M. Y. Zhang, K. E. Thummel, and P. B. Watkins. Identification of a novel route of extraction of sirolimus in human small intestine: roles of metabolism and secretion. *J. Pharmacol. Exp. Ther.* **301**:174–186 (2002).
26. L. Z. Benet, S. Oie, and J. B. Schwartz. Design and Optimization of Dosage Regimens; Pharmacokinetic Data. In J. G. Hardman, L. E. Limbird, P. B. Molinoff, R. W. Ruddon and G.G.A. (eds), *Goodman and Gilman's The Pharmacological Basis of Therapeutics* (J. G. HardmanL. E. LimbirdP. B. Molinoff R. W. Ruddonand G. G. A., eds), McGraw-Hill, New York, 1990, pp. 1707–1792.
27. J. W. Polli, S. A. Wring, J. E. Humphreys, L. Huang, J. B. Morgan, L. O. Webster, and C. S. Serabjit-Singh. Rational use of in vitro P-glycoprotein assays in drug discovery. *J. Pharmacol. Exp. Ther.* **299**:620–628 (2001).
28. A. H. Schinkel. Pharmacological insights from P-glycoprotein knockout mice. *Int. J. Clin. Pharmacol. Ther.* **36**:9–13 (1998).
29. T. Terao, E. Hisanaga, Y. Sai, I. Tamai, and A. Tsuji. Active secretion of drugs from the small intestinal epithelium in rats by P-glycoprotein functioning as an absorption barrier. *J. Pharm. Pharmacol.* **48**:1083–1089 (1996).
30. M. D. Troutman and D. R. Thakker. Rhodamine 123 Requires Carrier-Mediated Influx for Its Activity as a P-glycoprotein Substrate in Caco-2 Cells. *Pharm. Res.* **20:**1192–1199 (2003).
31. M. D. Troutman and D. R. Thakker. The Efflux Ratio Cannot Assess P-glycoprotein-Mediated Attenuation of Absorptive Transport - Asymmetric Effect of P-glycoprotein on Absorptive and Secretory Transport Across Caco-2 Cell Monolayers. *Pharm Res.* **20:**1200–1209 (2003).
32. P. Schmiedlin-Ren, K. E. Thummel, J. M. Fisher, M. F. Paine, K. S. Lown, and P. B. Watkins. Expression of enzymatically active CYP3A4 by Caco-2 cells grown on extracellular matrix-coated permeable supports in the presence of 1alpha,25-dihydroxyvitamin D3. *Mol. Pharmacol.* **51**:741–754 (1997).
33. U. A. Germann, M. C. Willingham, I. Pastan, and M. M. Gottesman. Expression of the human multidrug transporter in insect cells by a recombinant baculovirus. *Biochemistry* **29**:2295–2303 (1990).
34. K. Lee and D. R. Thakker. Saturable transport of H2-antagonists ranitidine and famotidine across Caco-2 cell monolayers. *J. Pharm. Sci.* **88**:680–687 (1999).
35. M. J. Cho, D. P. Thompson, C. T. Cramer, T. J. Vidmar, and J. F. Scieszka. The Madin Darby canine kidney (MDCK) epithelial cell monolayer as a model cellular transport barrier. *Pharm. Res.* **6**:71–77 (1989).
36. O. H. Lowry, N. J. Rosebrough, A. L. Farr, and R. J. Randall. Protein measurement with the folin phenol reagent. *J. Biol. Chem.* **193**:265–275 (1951).
37. F. Hyafil, C. Vergely, P. Du Vignaud, and T. Grand-Perret. In vitro and in vivo reversal of multidrug resistance by GF120918, an acridonecarboxamide derivative. *Cancer Res.* **53**:4595–4602 (1993).
38. F. Ingels, S. Deferme, E. Destexhe, M. Oth, G. Van den Mooter, and P. Augustijns. Simulated intestinal fluid as transport medium in the Caco-2 cell culture model. *Int. J. Pharm.* **232**:183–192 (2002).
39. J. Gao, O. Murase, R. L. Schowen, J. Aube, and R. T. Borchardt. A functional assay for quantitation of the apparent affinities of ligands of P-glycoprotein in Caco-2 cells. *Pharm. Res.* **18**:171–176 (2001).
40. S. Doppenschmitt, H. Spahn-Langguth, C. G. Regardh, and P. Langguth. Role of P-glycoprotein-mediated secretion in absorptive drug permeability: An approach using passive membrane permeability and affinity to P-glycoprotein. *J. Pharm. Sci.* **88**:1067–1072 (1999).
41. N. F. Ho, P. S. Burton, R. A. Conradi, and C. L. Barsuhn. A biophysical model of passive and polarized active transport processes in Caco-2 cells: approaches to uncoupling apical and basolateral membrane events in the intact cell. *J. Pharm. Sci.* **84**:21–27 (1995).
42. S. H. Jang, M. G. Wientjes, and J. L. Au. Kinetics of P-glycoprotein-mediated efflux of paclitaxel. *J. Pharmacol. Exp. Ther.* **298**:1236–1242 (2001).
43. K. A. Lentz, J. W. Polli, S. A. Wring, J. E. Humphreys, and J. E. Polli. Influence of passive permeability on apparent P-glycoprotein kinetics. *Pharm. Res.* **17**:1456–1460 (2000).
44. C. Martin, G. Berridge, C. F. Higgins, P. Mistry, P. Charlton, and R. Callaghan. Communication between multiple drug binding sites on P-glycoprotein. *Mol. Pharmacol.* **58**:624–632 (2000).
45. M. Horio, K. V. Chin, S. J. Currier, S. Goldenberg, C. Williams, I. Pastan, and M. M. Gottesman. and J. Handler. Transepithelial transport of drugs by the multidrug transporter in cultured Madin-Darby canine kidney cell epithelia. *J. Biol. Chem.* **264**:14880–14884 (1989).
46. Y. Zhang and L. Z. Benet. Characterization of P-glycoprotein mediated transport of K02, a novel vinylsulfone peptidomimetic cysteine protease inhibitor, across MDR1- MDCK and Caco-2 cell monolayers. *Pharm. Res.* **15**:1520–1524 (1998).
47. S. Ito, C. Woodland, B. Sarkadi, G. Hockmann, S. E. Walker, and G. Koren. Modeling of P-glycoprotein-involved epithelial drug transport in MDCK cells. *Am. J. Physiol.* **277**:F84–F96 (1999).
48. C. J. Matheny, M. W. Lamb, K. R. Brouwer, and G. M. Pollack. Pharmacokinetic and pharmacodynamic implications of P-glycoprotein modulation. *Pharmacotherapy* **21**:778–796 (2001).
49. W. D. Stein. Kinetics of the P-glycoprotein, the multidrug transporter. *Exp. Physiol.* **83**:221–232 (1998).
50. D. R. Ferry, P. J. Malkhandi, M. A. Russell, and D. J. Kerr.

Allosteric regulation of [3H]vinblastine binding to P-glycoprotein of MCF-7 ADR cells by dexniguldipine. *Biochem. Pharmacol.* **49**:1851–1861 (1995).
51. R. Liu and F. J. Sharom. Site-directed fluorescence labeling of P-glycoprotein on cysteine residues in the nucleotide binding domains. *Biochemistry* **35**:11865–11873 (1996).
52. C. Martin, G. Berridge, C. F. Higgins, and R. Callaghan. The multi-drug resistance reversal agent SR33557 and modulation of vinca alkaloid binding to P-glycoprotein by an allosteric interaction. *Br. J. Pharmacol.* **122**:765–771 (1997).
53. C. Martin, G. Berridge, P. Mistry, C. Higgins, P. Charlton, and R. Callaghan. Drug binding sites on P-glycoprotein are altered by ATP binding prior to nucleotide hydrolysis. *Biochemistry* **39**: 11901–11906 (2000).
54. K. Simons and S. D. Fuller. Cell surface polarity in epithelia. *Annu. Rev. Cell Biol.* **1**:243–288 (1985).
55. K. Simons and G. van Meer. Lipid sorting in epithelial cells. *Biochemistry* **27**:6197–6202 (1988).
56. I. Chantret, A. Barbat, E. Dussaulx, M. G. Brattain, and A. Zweibaum. Epithelial polarity, villin expression, and enterocytic differentiation of cultured human colon carcinoma cells: a survey of twenty cell lines. *Cancer Res.* **48**:1936–1942 (1988).
57. C. Le Grimellec, G. Friedlander, E. H. el Yandouzi, P. Zlatkine, and M. C. Giocondi. Membrane fluidity and transport properties in epithelia. *Kidney Int.* **42**:825–836 (1992).
58. C. Le Grimellec, G. Friedlander, and M. C. Giocondi. Asymmetry of plasma membrane lipid order in Madin-Darby Canine Kidney cells. *Am. J. Physiol.* **255**:F22–F32 (1988).